
CLIP-RR: IMPROVED CLIP NETWORK FOR RELATION-FOCUSED CROSS-MODAL INFORMATION RETRIEVAL

Yan Gong, Georgina Cosma
 Department of Computer Science
 Loughborough University
 Loughborough
 {y.gong2, g.cosma}@lboro.ac.uk

ABSTRACT

Relation-focused cross-modal information retrieval focuses on retrieving information based on relations expressed in user queries, and it is particularly important in information retrieval applications and next-generation search engines. To date, CLIP (Contrastive Language-Image Pre-training) achieved state-of-the-art performance in cross-modal learning tasks due to its efficient learning of visual concepts from natural language supervision. However, CLIP learns visual representations from natural language at a global level without the capability of focusing on image-object relations. This paper proposes a novel CLIP-based network for Relation Reasoning, CLIP-RR, that tackles relation-focused cross-modal information retrieval. The proposed network utilises CLIP to leverage its pre-trained knowledge, and it additionally comprises two main parts: (1) extends the capabilities of CLIP to extract and reason with object relations in images; and (2) aggregates the reasoned results for predicting the similarity scores between images and descriptions. Experiments were carried out by applying the proposed network to relation-focused cross-modal information retrieval tasks on the RefCOCOg, CLEVR, and Flickr30K datasets. The results revealed that the proposed network outperformed various other state-of-the-art networks including CLIP, VSE ∞ , and VSRN++ on both image-to-text and text-to-image cross-modal information retrieval tasks.

Keywords visual semantic embedding network, cross-modal, information retrieval, relation reasoning.

1 Introduction

Cross-modal information retrieval, and in particular image-to-text and text-to-image retrieval, has become increasingly important in real-world applications due to the growth of multi-modal multi-media data [1]. Current works utilise Visual-Semantic Embedding (VSE) networks to embed image–description pairs in the same latent space, and compute the similarity scores of pairs for retrieval tasks [2]. Relation-focused cross-modal information retrieval focuses on retrieving information based on relations expressed in user queries, and it is particularly important in information retrieval applications and next-generation search engines. Such capability will result in improved retrieval and ranking performance since the results will be more relevant to the user’s query than when relations are not considered. Consider for example Figure 1 that shows a description query that contains relations, i.e. ‘person walking with food’, a system that considers object relations will rank images (e.g. Figure 1(a)) with a person holding food as more similar to the query than images (e.g. Figure 1(b)) with people and food.

State-of-the-art VSE networks can align images and descriptions, creating visual representations from natural language, and they have been used in cross-modal retrieval but not for relation-focused retrieval. Faghri et al. [3] proposed a hard negatives loss function to optimise their network for learning the alignment between the representations of image and description. Lee et al. [4] explore the alignment between images and descriptions at the object–word level, and Li et al. [5] employ a GCN to extract the relations between image objects for obtaining high-level visual semantics. Chen et al. [6] applied the pre-trained Bidirectional Encoder Representations from Transformers (BERT [7]) network

Query: *Girl walking with food.*



Figure 1: A retrieval system that considers object relations will rank the image (a) of ‘a person holding food’ as more relevant to the query description than the image (b) of just ‘people and food’.

for cross-modal information retrieval. Recently, Radford et al. [8] proposed a Contrastive Language-Image Pre-training network (CLIP) which achieved state-of-the-art performance in cross-modal tasks. CLIP employs the pre-trained GPT-2 and Visual Transformer (ViT) to encode descriptions and images into a shared embedding space respectively [8], and has been widely applied to various information retrieval tasks such as e-commerce image retrieval [9], and text-image generation [10]. One of CLIP’s limitations is that it cannot identify relations between objects in images. CLIP is trained to match an image with the relevant description at the global level, therefore it is unaware of the alignment between image objects and textual descriptions [11]. Furthermore, compared to the Convolutional Neural Network (CNN), although CLIP’s ViT (Visual Transformer) has excellent global representation ability it weakly considers the local information of an image [12].

This paper proposes CLIP-RR, a novel network that performs Relation Reasoning in images, and which extends CLIP’s capabilities in extracting and reasoning about relations between objects within images. In this paper, relation reasoning refers to the extraction of relations between image objects that are relevant to a textual description, followed by the generation of the relation-focused local representations of the image that aim to enhance cross-modal information retrieval performance. The contributions of the paper are as follows.

- The proposed CLIP-RR network benefits from pre-trained knowledge of CLIP (consisting of ViT and GPT-2) to derive the global representation of image and description pairs. CLIP-RR uses a CNN encoder to determine the local representations of image and description pairs. Both global and local representations are finally aggregated by CLIP-RR and utilised to predict the similarity scores of image and description pairs.
- To address the task of relation-focused cross-modal information retrieval, CLIP-RR leverages a novel relation reasoning module that first models an image’s objects and their relations using a relational graph, then generates local representations aligned with the image’s description. Using CLIP-RR’s relation-focused local image representations, cross-modal information retrieval performance is improved.
- Extensive experiments were carried out by applying the CLIP-RR to three datasets RefCOCOg, CLEVR and Flickr30K. CLIP-RR outperformed various other state-of-the-art networks including CLIP, VSRN++, and VSE ∞ on both image-to-text and text-to-image cross-modal information retrieval tasks.

2 Related Work

2.1 Visual Semantic Embedding

Faghri et al. [3] proposed an improved Visual-Semantic Embedding architecture called VSE++. VSE++ uses a fully connected neural network and a Gated Recurrent Units (GRU) network [13] to embed both the image features (extracted by the faster R-CNN [14]) and the description as representations respectively. Liu et al. [15] used a variant of the triplet loss function in their novel VSE network for cross-modal information retrieval, replacing the input text embedding with the reconstructed image embedding of the network. Lee et al. [4] proposed a stacked cross attention network that discovers the full latent alignments between image objects and descriptive words to infer the similarity of image–description pairs. Li et al. [5] introduced the Visual Semantic Reasoning Network (VSRN) to enhance image features with image object relations extracted by a GCN [16]. Later, Li et al. [17] improved the VSRN by upgrading it to VSRN++, which replaces the word2vector embeddings with pre-trained BERT embeddings. Chen et al. [6] proposed a variation of the VSE network, VSE ∞ , that benefits from a generalised pooling operator which discovers the best strategy for pooling image and description representations. However, none of the above networks specifically focus on exploring relation reasoning for cross-modal information retrieval tasks.

2.2 The Network of CLIP

Radford et al. [8] proposed the pre-trained CLIP which applies contrastive learning to align the global visual representations and textual representations from a dataset including 400 million image–description pairs. The architecture of CLIP involves: (1) a text encoder of GPT-2 aims to embed the description as a dimension-reduced representation; (2) an image encoder, commonly using ViT, aims to embed the image as a representation with the same dimension as the description representation. Radford et al. [8] also provided a CNN version of the image encoder. However, due to the advantage of ViT on pre-training, the ViT encoder outperformed the CNN encoder, and it is most commonly applied in other works [9]. CLIP has recently been used in various tasks, such as e-commerce image retrieval [9], text-image generation [10], and image segmentation [18]. However, CLIP still lacks the ability to effectively match local information in images to their descriptions in cross-modal information retrieval tasks [12].

2.3 Relation Reasoning Methods

In recent years, graph-based methods have shown an efficient way of reasoning with vision relations [19]. Yu et al. [19] proposed a network based on both the visual and semantic graphs for visual question answering. For a scene graph generation task, Lin et al. [20] explored the atom correlation-based graph propagation which incorporates prior knowledge in a more stable and comprehensive way. For cross-modal information retrieval, Cao et al. [21] introduced a graph-based relation-aware attention module to weigh image fragments based on the pairwise relations of the fragments; and Li et al. [17] applied a GCN to extract relations between image objects, and used the extracted relations to enhance image features. Although graph-based networks are established and efficient for reasoning about relations, they are less utilised by pre-trained cross-modal networks, such as CLIP, for information retrieval tasks.

3 The Proposed CLIP-Relation Reasoning (CLIP-RR) Network

Overview. The proposed CLIP-RR network is illustrated in Figure 2. Given an image I and a description D , CLIP-RR aims to embed the pair into the shared latent space for predicting the pair’s similarity score $s(I, D)$. CLIP-RR is comprised of: (1) A ViT encoder and a GPT-2 encoder, that encode an image I and its description D respectively to provide pre-trained knowledge. (2) A CNN that encodes objects in an image I as a set of features V . (3) A relation reasoning module that represents image objects in relations using a block of modeling relations, and generates local representations of the image objects based on their descriptions using a block of aligning text-image. (4) An aggregation module that predicts the similarity score $s(I, D)$ based on aggregating the results of CLIP-RR’s relation reasoning module and pre-trained knowledge using a Graph Neural Network (GNN) [22] and a GRU network.

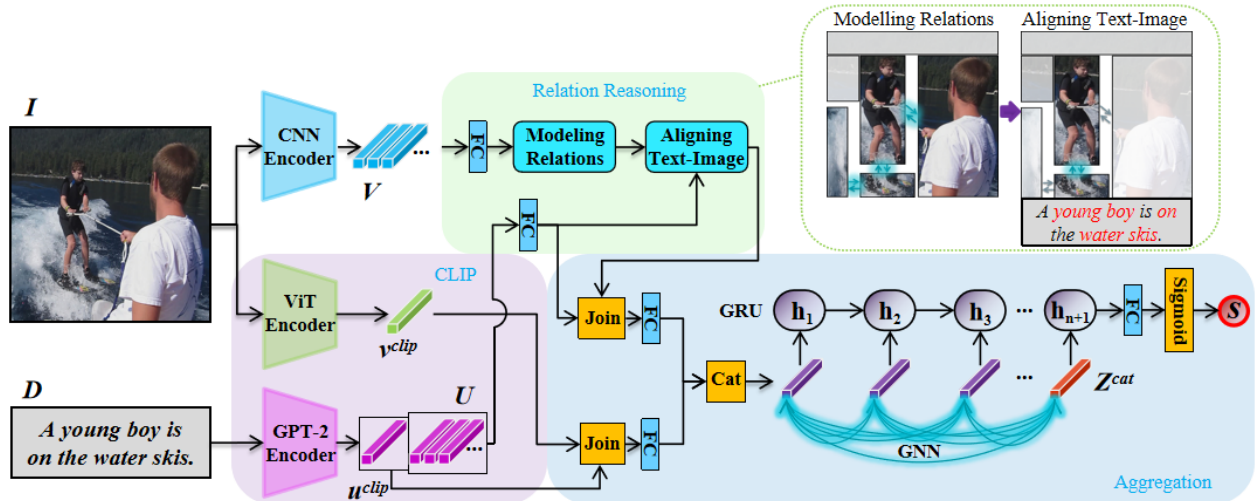


Figure 2: An overview of the proposed CLIP-RR. CLIP-RR consists of: (1) pre-trained ViT and GPT-2 encoders from CLIP that provide pre-trained knowledge of an image and its description, respectively; (2) a CNN encoder that extracts features from objects; (3) a *Relation Reasoning* module that models the relations between objects in an image and generates local representations of the objects based on their descriptions; and (4) an *Aggregation* module that aggregates the outputs from Relation Reasoning and pre-trained knowledge through GNN and GRU networks, and outputs the similarity score between the image I and description D .

3.1 Obtaining Pre-trained Knowledge

CLIP-RR integrates CLIP [8] for gaining pre-trained knowledge. The pre-trained knowledge is provided as follows: (1) CLIP’s ViT encoder encodes image I as a global representation vector $v^{clip} \in \mathbb{R}^{d_1}$; (2) CLIP’s GPT-2 encoder encodes description D as a global representation vector $u^{clip} \in \mathbb{R}^{d_1}$, and a set of word embedding vectors $U = \{u_j | u_j \in \mathbb{R}^{d_1}\}_{j=1}^n$, where n is the number of descriptive words, and u_j is the j th word embedding vector with dimension d_1 . The outputs of this module are the set U and vectors v^{clip} and u^{clip} .

3.2 Encoding Image Objects

CLIP-RR uses a CNN encoder (e.g. the pre-trained Resnet) to encode the objects of the image I as a set of features $V = \{v_i | v_i \in \mathbb{R}^{d_2}\}_{i=1}^k$, where k is the number of objects, and vector v_i with dimension d_2 is the feature of the i th object. The output of this module is the set V .

3.3 Relation Reasoning

Preparation for Unifying the Dimensions of Vectors. Vectors in the sets V and U are projected into a unified dimension d_3 as shown in Eq. (1):

$$\begin{aligned} V^* &= W^v(V), \\ U^* &= W^u(U), \end{aligned} \quad (1)$$

where the weight parameters W^v and W^u are both the fully connected layers with d_3 output neurons. $V^* = \{v_i^* | v_i^* \in \mathbb{R}^{d_3}\}_{i=1}^k$ is a set of the projected vectors, where v_i^* with dimension d_3 is the vector corresponding to the i th object. $U^* = \{u_j^* | u_j^* \in \mathbb{R}^{d_3}\}_{j=1}^n$ is a set of projected word embedding vectors, where u_j^* is the j th vector with dimension d_3 .

Modeling Relations. This block represents an image’s objects and their relations extracted from the relational graph. Let R be a matrix of relations of objects and computed as Eq. (2):

$$R = W^{\varphi_1}(V^*)W^{\phi_1}(V^*)^T, \quad (2)$$

where the weight parameters W^{φ_1} and W^{ϕ_1} are both the fully connected layers with d_3 output neurons, and $R \in \mathbb{R}^{k \times k}$. According to R , the matrix of pairwise relations of objects, R^{pr} , is computed as Eq. (3):

$$R^{pr} = \sigma(W^{R_1}(cat[R^T, R])), \quad (3)$$

where cat and σ denote the concatenating operation and the $Tanh$ activation function respectively, $cat[R^T, R] \in \mathbb{R}^{2k \times k}$, the weight parameter W^{R_1} is a 1D convolutional layer (kennel size 1 and k output channels), and $R^{pr} \in \mathbb{R}^{k \times k}$. Additionally, let set R^s hold the inner information for each vector in set V^* , and be computed as Eq. (4):

$$R^s = \sigma(W^{R_2}(V^*)), \quad (4)$$

where the weight parameter W^{R_2} is a fully connected layer with 1 output neuron, and $R^s \in \mathbb{R}^{k \times 1}$. Merging R^{pr} and R^s into a matrix R^f as Eq. (5):

$$R^f = \sigma(W^{R_3}(cat[R^{pr}, R^s])), \quad (5)$$

where $cat[R^{pr}, R^s] \in \mathbb{R}^{k \times (k+1)}$, the weight parameter W^{R_3} is a fully connected layer with 1 output neuron, and $R^f \in \mathbb{R}^{k \times 1}$. Let $R^f \in \mathbb{R}^{k \times 1}$ be expanded as $R^{f_d} \in \mathbb{R}^{k \times d_3}$, therefore the weight matrix Q is computed as Eq. (6):

$$Q = sigmoid(R^{f_d}), \quad (6)$$

where the sigmoid function normalises R^{f_d} into values of $[0, 1]$. The represented vectors set V^a is obtained by multiplying V^* with Q , as Eq. (7):

$$V^a = QV^*, \quad (7)$$

V^a is defined as $V^a = \{v_i^a | v_i^a \in \mathbb{R}^{d_3}\}_{i=1}^k$, where v_i^a is the represented vector corresponding to the i th object. Furthermore, the block of modeling relations can be iteratively operated for $g_1 \in \mathbb{N}^+$ steps, where the output V^a from the last step is taken as the input for the next step.

Aligning Text-Image. This block weighs the vectors in set V^a to generate the image’s local representations which are aligned with the descriptive words. Let $s(v_i^a, u_j^*)$ denote the cosine similarity between the i th represented vector v_i^a and the j th projected word embedding vector u_j^* , and its normalisation value $\bar{s}(v_i^a, u_j^*)$ is computed as Eq. (8):

$$\bar{s}(v_i^a, u_j^*) = [s(v_i^a, u_j^*)]_+ / \sqrt{\sum_{j=1}^n [s(v_i^a, u_j^*)]_+^2}, \quad (8)$$

where $[x]_+ \equiv \max(x, 0)$. Then the weight for v_i^a is computed by Eq. (9):

$$a_{ij} = \text{softmax}(\gamma \bar{s}(v_i^a, u_j^*)), \quad (9)$$

where the weight a_{ij} is calculated from $\bar{s}(v_i^a, u_j^*)$ by using a softmax function with a temperature parameter γ (set 12 by this paper). Then the newly generated image local representation vector v_j^r being aligned with the j th word is obtained as Eq. (10):

$$v_j^r = \sum_{i=1}^k a_{ij} v_i^a. \quad (10)$$

Set $V^r = \{v_j^r | v_j^r \in \mathbb{R}^{d_3}\}_{j=1}^n$ is obtained by operating Eq. (10) for all v_i^a in set V^a , where v_j^r is the j th generated image local representation vector being aligned with the j th word. The output of relation reasoning are sets V^r and U^* .

3.4 Aggregation

This module predicts the similarity score $s(I, D)$ for the image–description pair by aggregating the results of the relation reasoning module and pre-trained knowledge. The process is described as follows.

Joining Image–Description Representations. Let z^{clip} denote a vector for joining a global image–description representation pair (v^{clip}, u^{clip}) , and let z_j^{rr} denote a vector for joining a local image–description representation pair (v_j^r, u_j^*) . z^{clip} and z_j^{rr} are computed as Eq. (11):

$$\begin{aligned} z^{clip} &= |u^{clip} - v^{clip}|^2, \\ z_j^{rr} &= |u_j^* - v_j^r|^2, \end{aligned} \quad (11)$$

where $|\cdot|^2$ indicates the computation of euclidean distances at the element level between two vectors. Thereafter, let $Z^{rr} = \{z_j^{rr} | z_j^{rr} \in \mathbb{R}^{d_3}\}_{j=1}^n$ denote a set of the joined vectors for set $\{(v_j^r, u_j^*)\}_{j=1}^n$, then Eq. (12) concatenates z^{clip} into set Z^{rr} :

$$Z^{cat} = \text{cat}[W^{rr}(Z^{rr}), W^{clip}(z^{clip})], \quad (12)$$

where the weight parameters W^{rr} and W^{clip} are both the fully connected layers with d_4 output neurons, and $Z^{cat} \in \mathbb{R}^{(n+1) \times d_4}$. The result of Eq. (12) is a set of joined vectors of image–description representations, and denoted as $Z^{cat} = \{z_j^{cat} | z_j^{cat} \in \mathbb{R}^{d_4}\}_{j=1}^{n+1}$, where z_j^{cat} is the j th joined vector.

GNN for Aggregating Joined Vectors. Each vector z_j^{cat} in set Z^{cat} can be treated as the node to build a graph, and the edge matrix E is obtained as Eq. (13):

$$E = W^{\varphi_2}(Z^{cat})W^{\phi_2}(Z^{cat})^T, \quad (13)$$

where the weight parameters W^{φ_2} and W^{ϕ_2} are both fully connected layers with d_4 output neurons. Then the GNN is applied to aggregate the information among the joined vectors as Eq. (14):

$$Z^{agg} = W^{agg}(\text{sigmoid}(E)Z^{cat}), \quad (14)$$

where $\text{sigmoid}(E)$ computes the weights for Z^{cat} , and the weight parameter W^{agg} is a fully connected layer with d_4 output neurons. Z^{agg} is defined as $Z^{agg} = \{z_j^{agg} | z_j^{agg} \in \mathbb{R}^{d_4}\}_{j=1}^{n+1}$, where z_j^{agg} is the j th aggregated vector from z_j^{cat} . Furthermore, Eq. (13)~Eq. (14) can be iteratively operated for $g_2 \in \mathbb{N}^+$ steps, where the output Z^{agg} from the last step is taken as the input for the next step.

GRU for Pooling Joined Vectors. Since Z^{agg} is a sequence of vectors with uncertain lengths $(n + 1)$, the GRU network is applied for pooling the sequence as Eq. (15):

$$\{h_j\}_{j=1}^{n+1} = \text{GRU}(\{z_j^{agg}\}_{j=1}^{n+1}), \quad (15)$$

where $\{h_j\}_{j=1}^{n+1}$ is the hidden states of the GRU network, and only h_1 is taken as the result.

Predicting Image–Description Similarity Score. The similarity score s for pair (I, D) is predicted as Eq. (16):

$$s = \text{sigmoid}(W^h(h_1)), \quad (16)$$

where the weight parameter W^h is a fully connected layer with 1 output neuron, and the result $s(I, D) \in [0, 1]$ is predicted by the sigmoid function with the input h_1 weighted by W^h .

3.5 Training CLIP-RR

The ViT, GPT-2, and CNN encoders are taken from pre-trained models and the remaining parameters of CLIP-RR are jointly trained using the improved Semantically-Enhanced Hard Negatives Loss function (LSEH) [23]. LSEH is an improved version of the hard negatives loss function [3] in terms of training efficiency. Let $\{(I_p, D_p)\}_{p=1}^m$ denote a training set containing paired images and descriptions, where each image I_p corresponds to its relevant description D_p , p is the index, and m is the size of the training set. Given a relevant image–description pair (I_p, D_p) , the result of LSEH only takes the max from the irrelevant pairs as Eq. (17):

$$\begin{aligned} L(I_p, D_p) = & \max_{\hat{D}_p} [\alpha + F + s(I_p, \hat{D}_p) - s(I_p, D_p)]_+ \\ & + \max_{\hat{I}_p} [\alpha + F + s(D_p, \hat{I}_p) - s(I_p, D_p)]_+, \end{aligned} \quad (17)$$

where $F = \lambda s_{cs}(D'_p, \hat{D}'_p)$,

where $[x]_+ \equiv \max(x, 0)$, and α (set to 0.185) serves as a margin parameter. Let $s(I_p, D_p)$ be the similarity score between the relevant image I_p and description D_p ; let $s(I_p, \hat{D}_p)$ be the set of similarity scores of the image I_p with all its irrelevant descriptions \hat{D}_p ; and let $s(D_p, \hat{I}_p)$ be the set of similarity scores of the descriptions D_p with all its irrelevant image representations \hat{I}_p . Additionally, let D'_p and \hat{D}'_p be the decomposition eigenvalues of D_p and \hat{D}_p respectively, λ (set to 0.025) serves as a temperature hyperparameter, then the semantic factors F dynamically adjust the margin α according to the cosine similarity (s_{cs}) between D'_p and \hat{D}'_p for a flexible learning of the network. D'_p and \hat{D}'_p are obtained as follows:

Let the training description set $\{D_p\}_{p=1}^m$ convert to a matrix A of size $m \times w$, where m is the number of descriptions, w is the total number of unique terms found in the set of descriptions, then the truncated SVD is applied to $A_{m \times w}$ as shown in Eq. (18):

$$\begin{aligned} A_{m \times w} & \approx X_{m \times d_5} \Lambda_{d_5 \times d_5} Y_{d_5 \times w}^T, \\ B_{m \times d_5} & = A_{m \times w} Y_{w \times d_5}, \end{aligned} \quad (18)$$

where d_5 is the number of singular values. The matrix B contains m rows of decomposition eigenvalues (d_5 dimension) and it is obtained by multiplying the original descriptions matrix $A_{m \times w}$ with the matrix $Y_{w \times d_5}$. Let $\{D'_p | D'_p \in \mathbb{R}^{d_5}\}_{p=1}^m$ denote a set of decomposition eigenvalues converted from matrix $B_{m \times d_5}$, therefore D'_p and \hat{D}'_p are taken from the set. Furthermore, z^{clip} has been pre-trained by CLIP, while Z^{rr} has not, to avoid learning bias, Z^{rr} should be trained individually before merging with z^{clip} . Therefore, a condition hyperparameter η is introduced to Eq. (12) as follow:

$$\begin{aligned} Z^{cat} & = \text{cat}[W^{rr}(Z^{rr}), W^{clip}(z^{clip})] \text{ if } \text{epochs} \geq \eta, \\ Z^{cat} & = W^{rr}(Z^{rr}) \text{ if } \text{epochs} < \eta. \end{aligned} \quad (19)$$

4 Experiments

The proposed CLIP-RR was evaluated for the tasks of image-to-text and text-to-image retrieval using the RefCOCOg [24], CLEVR [25], and Flickr30K [26] datasets. The performance of CLIP-RR is compared to state-of-the-art VSE networks, namely CLIP [8], VSE ∞ [6], and VSRN++ [17].

4.1 Evaluation Measures

The evaluation measure that was utilised for the cross-modal information retrieval experiments is the commonly used Recall at rank k (Recall@k), which is defined as the percentage of relevant items in the top k retrieved results [2]. The experiments evaluate the performance of the network in retrieving any one of the relevant items from the list of relevant items and use average Recall among the results of the tested queries.

4.2 Datasets

The RefCOCOg, CLEVR, and Flickr30K datasets are split as shown in Table 1 and described as follows.

Table 1:
Dataset split of RefCOCOg, CLEVR, and Flickr30K.

Dataset		Train	Validate	Test
RefCOCOg	images	21899	1300	2600
	descriptions	80512	4896	9582
CLEVR	images	30000	1000	1000
	descriptions	98345	3136	3121
Flickr30K	images	29000	1000	1000
	descriptions	145000	5000	5000

The **RefCOCOg** dataset [24] contains real-world images taken from the MS-COCO dataset [27] and their corresponding descriptions provided by the University of Maryland (UMD). The UMD descriptions contain information on relations between objects in images. On average, each image in the dataset is associated with four relevant descriptions.

The **CLEVR (Compositional Language and Elementary Visual Reasoning)** [25] dataset contains images of 3D-rendered objects annotated with four relations ('left', 'right', 'front', and 'behind'). CLEVR has not been used for relation-focused cross-modal retrieval, so the image descriptions were generated from provided annotations. The dataset was then split into train, test, and validation sets. The prepared image descriptions and the indices of the images found in the train, test, and validation sets are provided in our GitHub repository for experiment reproducibility purposes. On average, each CLEVR image is associated with three relevant descriptions. An example description is 'A large blue metal cube is behind a large blue rubber sphere'.

The **Flickr30K** dataset [26] is a commonly used benchmark for evaluating the performance of VSE networks [8, 6, 17]. Each image in the dataset is associated with five textual descriptions.

4.3 Implementation Details

All experiments were conducted on a workstation with NVIDIA RTX3090 GPU with PyTorch framework, and the source code files of the experiments are provided in our GitHub repository. The networks were implemented as follows.

Baselines: CLIP models. Three CLIP baseline models were selected. These were the base ViT model ('ViT-B/16' with dimension d_1 of 512), the large ViT model ('ViT-L/14' with dimension d_1 of 768), and the Resnet101 model ('RN101') [8] denoted as CLIP_{B16}, CLIP_{L14}, and CLIP_{RN101} respectively. Each model was fine-tuned for each dataset to present its best performance, and the hyperparameter settings follow each model's benchmark settings [8].

Experiment Setup of CLIP-RR. CLIP-RR was implemented with two fine-tuned baseline models, namely CLIP_{B16} and CLIP_{L14} respectively, which were part of CLIP-RR. This resulted in two variations of CLIP-RR network, namely CLIP-RR_{B16} and CLIP-RR_{L14}, respectively. The image encoder of the fine-tuned CLIP_{RN101} was applied for encoding image objects for both CLIP-RR_{B16} and CLIP-RR_{L14}, and it extracts 49 features (with dimension d_2 of 2048) of objects from each image. Architecture settings of CLIP-RR_{B16} and CLIP-RR_{L14} are as Table 2. On each dataset, both CLIP-RR_{B16} and CLIP-RR_{L14} were trained for 20 epochs with a batch size of 128, the learning rate was set to 0.0004 with a decay of 0.1 at the 5th epoch, a condition η of 3 was set, and the Adam optimizer was applied.

Table 2:
Architecture settings of CLIP-RR_{B16} and CLIP-RR_{L14}.

Network	d_3	d_4	g_1	g_2
CLIP-RR _{B16}	1024	128	4	2
CLIP-RR _{L14}	2048	128	4	2

Additional Baselines. Two VSE networks were selected as additional baselines: (1) VSE ∞ is a state-of-the-art representations pooling network [6]; and (2) VSRN++ is a state-of-the-art reasoning image relations network [17]. Those two networks were implemented and tuned to achieve their best performance on the RefCOCOg and CLEVR datasets. For a fair comparison, the two networks used the same extracted features of image objects as CLIP-RR. The hyperparameters of each network for the RefCOCOg and CLEVR datasets refer to each network's benchmark settings for the Flickr30K dataset [6, 17].

4.4 Results and Analysis

Results on RefCOCOg. Table 3 compares the proposed CLIP-RR with the baseline methods on the RefCOCOg test set for cross-modal information retrieval, and the main findings are described as follows. CLIP-RR_{L14} reached a Recall@1 of 45.8% for image-to-text, and a Recall@1 of 29.5% for text-to-image retrieval. Observing the performance of the networks using the Recall@1 metric, CLIP-RR_{L14} outperformed CLIP_{L14} by 3.4% and 4.3% for image-to-text and text-to-image retrieval respectively, and also outperformed VSE ∞ by 14.7% and 10% for those tasks, respectively. CLIP-RR_{B16} reached a Recall@1 of 42.9% and 27.9% for image-to-text and text-to-image retrieval respectively, and outperformed CLIP_{B16} by 3.6% and 4.1% for those tasks, respectively.

Table 3:

Results of cross-modal information retrieval networks on the RefCOCOg test set. Table shows average Recall@ k (%) values.

Network	Image-to-Text			Text-to-Image		
	Recall@1	Recall@5	Recall@10	Recall@1	Recall@5	Recall@10
VSRN++	20.0	44.9	57.3	13.8	34.6	47.8
VSE ∞	31.1	58.3	69.7	19.5	42.8	55.2
CLIP _{RN101}	36.3	61.3	71.2	20.8	44.2	56.7
CLIP _{B16}	39.3	64.3	75.0	23.8	48.4	60.4
CLIP _{L14}	42.4	65.5	75.1	25.2	48.9	60.4
CLIP-RR _{B16} (ours)	42.9	68.2	79.2	27.9	53.5	65.6
CLIP-RR _{L14} (ours)	45.8	72.2	80.7	29.5	54.9	66.5

Table 4:

Results of cross-modal information retrieval networks on the CLEVR test set. Table shows average Recall@ k (%) values.

Network	Image-to-Text			Text-to-Image		
	Recall@1	Recall@5	Recall@10	Recall@1	Recall@5	Recall@10
VSRN++	64.3	96.9	99.4	58.5	91.0	96.1
CLIP _{RN101}	65.4	98.1	99.8	61.8	95.7	98.1
CLIP _{L14}	65.6	99.4	99.9	65.2	97.6	99.1
CLIP _{B16}	66.8	98.6	100.0	65.5	97.8	99.5
VSE ∞	67.8	99.7	99.9	70.8	99.0	99.5
CLIP-RR _{B16} (ours)	88.3	99.7	100.0	79.4	99.4	99.8
CLIP-RR _{L14} (ours)	90.7	99.9	99.9	79.3	99.5	99.7

Results on CLEVR. Table 4 compares CLIP-RR with the baseline methods on the CLEVR test set for cross-modal information retrieval, and the main findings are described as follows. For CLIP-RR_{L14}, Recall@1 reached 90.7% for image-to-text and 79.3% for text-to-image retrieval, and outperformed CLIP_{L14} by 25.1% and 14.1% for those tasks respectively. CLIP-RR_{L14}’s Recall@1 also outperformed VSE ∞ ’s Recall@1 by 22.9% and 8.5% for image-to-text and text-to-image retrieval respectively. The Recall@1 values of CLIP-RR_{B16} were 88.3% and 79.4% for image-to-text and text-to-image retrieval respectively. The Recall@1 values of CLIP-RR_{B16} outperformed that of CLIP_{B16} by 21.5% for image-to-text and 13.9% for text-to-image retrieval respectively.

Results on Flickr30K. Table 5 reveals the performance of the proposed CLIP-RR on the Flickr30K test set for cross-modal information retrieval, and the main findings are described as follows. CLIP-RR_{L14}’s Recall@1 values for image-to-text and text-to-image retrieval achieved 94.7% and 82.5% respectively. CLIP-RR_{L14}’s Recall@1 values outperformed CLIP_{L14}’s Recall@1 values by 2.1% and 4.7% for image-to-text and text-to-image retrieval respectively. Furthermore, CLIP-RR_{L14}’s Recall@1 values also outperformed COTS † ’s Recall@1 values by 3.0% for image-to-text and 4.2% for text-to-image retrieval. CLIP-RR_{B16} reached the Recall@1 of 93.7% and 80.8% for image-to-text and text-to-image retrieval tasks respectively. The results of Recall@1 of CLIP-RR_{B16} outperformed that of CLIP_{B16} by 2.5% and 3.8% for image-to-text and text-to-image retrieval respectively.

Table 5:

Results of cross-modal information retrieval networks on the Flickr30K test set. Table shows average Recall@ k (%) values.

Network	Image-to-Text			Text-to-Image		
	Recall@1	Recall@5	Recall@10	Recall@1	Recall@5	Recall@10
VSE++ [3]	52.9	80.5	87.2	39.6	70.1	79.5
CycleMatch [15]	57.8	83.3	90.9	43.2	74.8	83.8
CAAN [28]	70.1	91.6	97.2	52.8	79.0	87.9
MMCA [29]	74.2	92.8	96.4	54.8	81.4	87.8
VSRN++ [17]	79.2	94.6	97.5	60.6	85.6	91.4
Unicoder [30]	86.2	96.3	99.0	71.5	90.9	94.9
Uniter [31]	87.3	98.0	99.2	75.6	94.1	96.8
ERNIE-ViL [32]	88.7	98.0	99.2	76.7	93.6	96.4
ViSTA-L [33]	89.5	98.4	99.6	75.8	94.2	96.9
CLIP _{RN101}	88.3	98.2	99.4	72.9	92.6	96.2
VILLA [34]	87.9	97.5	98.8	76.3	94.2	96.8
VSE ∞ [6]	88.7	98.9	99.8	76.1	94.5	97.1
CLIP _{B16}	91.2	98.9	99.4	77.0	94.1	97.4
COTS † [35]	91.7	99.0	99.9	78.3	94.9	97.2
CLIP _{L14}	92.6	99.2	99.6	77.8	95.2	97.7
CLIP-RR _{B16} (ours)	93.7	99.1	99.8	80.8	95.7	97.9
CLIP-RR _{L14} (ours)	94.7	99.7	99.9	82.5	96.7	98.3

4.5 Ablation Studies on the CLIP and Relation Reasoning Modules

This section performs ablation studies to evaluate the impact of the CLIP and relation reasoning modules of the proposed CLIP-RR network on relation-focused cross-modal information retrieval. Experiments were carried out by creating variants of CLIP-RR_{L14} and applying those to the RefCOCOg test set. The results of the experiments are shown in Table 6.

The aim of the first experiment is to evaluate the performance of the relation reasoning module when it does not utilise CLIP’s pre-trained knowledge, thereby evaluating the impact of CLIP on the network. For this experiment, a new variant of CLIP-RR_{L14} was created, namely RR_{L14}, that does not include the CLIP module. To generate the word embeddings, RR_{L14} uses GPT-2. RR_{L14} outperformed VSE ∞ for image-to-text and text-to-image on Recall@1, with average improvements of 5.0% and 4.8% respectively. In addition, RR_{L14} underperformed CLIP-RR_{L14} by 9.7% for image-to-text retrieval and 5.2% for text-to-image retrieval on Recall@1.

The aim of the second experiment is to evaluate the performance of CLIP-RR when the relation reasoning module is removed, thereby evaluating the impact of this module on the network. For this experiment, a new variant of CLIP-RR_{L14} was created, namely CLIP-GRU_{L14} that does not include the relation reasoning module. The relation reasoning module was replaced by two GRUs, one for pooling the text and another for pooling the object features of images. The results of Recall@1 of CLIP-GRU_{L14} outperformed that of CLIP_{L14} by 0.7% and 0.1% respectively, and the results suggest that this improvement is due to CLIP’s pre-trained knowledge being integrated into the network. Furthermore, it was observed that the performance of CLIP-GRU_{L14} was worse than that of CLIP-RR_{L14} by 2.7% and 4.2% for Recall@1 in image-to-text and text-to-image retrieval tasks, respectively.

5 Visualisation

5.1 Visually Representing the Relation Reasoning Performance of CLIP-RR

Figure 3 presents an example visualisation of relation reasoning generated by the proposed CLIP-RR. In Figure 3, the heat map highlights the image object regions relevant to the textual query, and it is generated by the relation reasoning module as follows.

Table 6:

Results of ablation studies on CLIP-RR’s variant networks for cross-modal information retrieval on the RefCOCOg test set. Table shows average Recall@ k (%) values.

Network	Image-to-Text			Text-to-Image		
	Recall@1	Recall@5	Recall@10	Recall@1	Recall@5	Recall@10
VSE ∞	31.1	58.3	69.7	19.5	42.8	55.2
RR L_{14}	36.1	61.6	72.2	24.3	49.1	60.8
CLIP L_{14}	42.4	65.5	75.1	25.2	48.9	60.4
CLIP-GRU L_{14}	43.1	66.7	76.9	25.3	49.3	60.4
CLIP-RR L_{14}	45.8	72.2	80.7	29.5	54.9	66.5

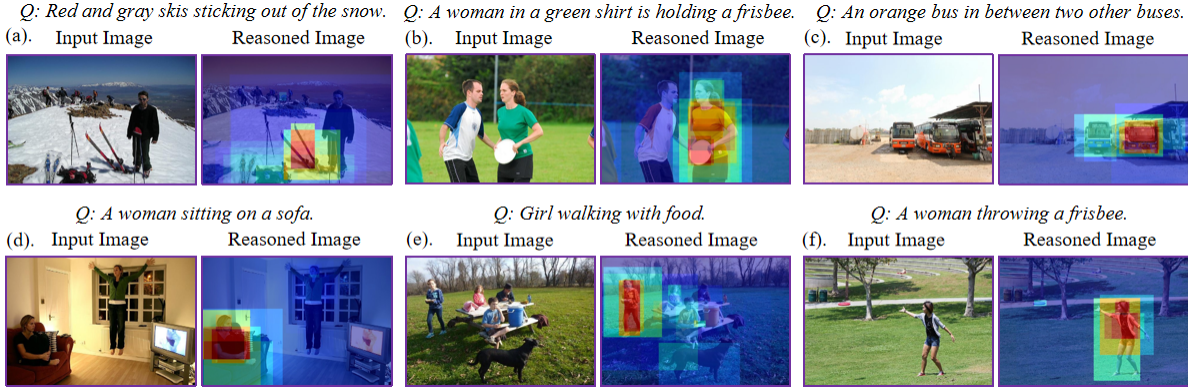


Figure 3: Visually representing the relation reasoning performance of CLIP-RR. In this figure, given a textual query (Q) and an input image, the visualisation is generated by highlighting the relevant image object regions and darkening the irrelevant image object regions.

Set $\{a_{ij}\}_{j=1}^n$ (see Eq. (9)) holds the weights for the i th image object. Let hd_i denote the average result of set $\{a_{ij}\}_{j=1}^n$ for the i th image object. Set $HD = \{hd_i\}_{i=1}^k$ holds the values of all image objects. Let set $\bar{HD} = \{\bar{hd}_i | \bar{hd}_i \in [0, 1]\}_{i=1}^k$ be the min-max normalisation result of set HD , and therefore \bar{hd}_i is used as the heat degree for the i th image object region.

The images from (a) to (f) in Figure 3 show that the image objects only received focus by the relation reasoning module when they were mentioned in the query description. For example, in Figure 3 (b), the image objects relevant to <‘woman’, ‘holding’, ‘frisbee’> were the focus, while the other main object ‘man’ in the image was ignored because it is irrelevant to the query description. The results of Figure 3 visually show the relation reasoning performance in CLIP-RR.

5.2 Visual Comparison of Retrieval Results between CLIP and CLIP-RR

Image-to-Text Retrieval. Figure 4 presents eight examples of the top two image-to-text retrieval results between CLIP and CLIP-RR. Typically, CLIP’s results offer a general description of the image, while CLIP-RR’s results concentrate on specific details. As seen in Figure 4 (b), CLIP describes the image as a class of ‘child’, while CLIP-RR describes it as a relation-focused sentence which is ‘a girl eating pizza’. Figure 4 highlights the limitations of CLIP in matching local image information, particularly relations, during image-to-text retrieval, and the improvement of CLIP-RR.

Text-to-Image Retrieval. Figure 5 presents two examples of the top two results of text-to-image retrieval between CLIP and CLIP-RR. As seen in Figure 5 (a), the intent of the query is to find an image of a cat resting on top of an object, but none of the results from CLIP are relevant to the description of the query. Conversely, CLIP-RR’s results are more relevant to the query. Figure 5 highlights the limitations of CLIP in matching relation information between images and descriptions during text-to-image retrieval, and the improvement of CLIP-RR.



Figure 4: A comparison of the top two results for image-to-text retrieval using CLIP and CLIP-RR. CLIP’s retrieved results typically provide a general description of the image, while CLIP-RR’s retrieved results concentrate on specific details of the image.



Figure 5: A comparison of the top two results for text-to-image retrieval using CLIP and CLIP-RR. None of CLIP’s results align with the description, whereas CLIP-RR’s results are more relevant to the query description.

6 Conclusion

This paper proposes a novel network for modeling the relations between objects in images for the task of cross-modal information retrieval. The proposed network, CLIP-RR, includes a relation reasoning module that extends the capabilities of CLIP by modeling the relations of objects in images for relation-focused cross-modal information retrieval; an aggregation module that aggregates the pre-trained knowledge of CLIP and the relation reasoned information of relation reasoning. In particular, CLIP-RR is re-purposing a large pre-trained network, CLIP, for relation-focused information retrieval. Empirical evaluations revealed that the proposed CLIP-RR network outperformed CLIP and other VSE networks for both relation-focused and traditional cross-modal information retrieval tasks. In terms of retrieval performance using the average Recall@1 evaluation metric, CLIP-RR outperformed CLIP by (1) 3.4% for image-to-text and 4.3% for text-to-image retrieval on the RefCOCOg dataset; (2) 25.1% for image-to-text and 14.1% for text-to-image retrieval on the CLEVR dataset; and (3) 2.1% for image-to-text and 4.7% for text-to-image retrieval on the Flickr30K dataset. Future work will apply CLIP-RR to other cross-modal information retrieval tasks (e.g. text-video retrieval), and extend CLIP-RR to search engine contexts.

References

- [1] Xin Shu and Guoying Zhao. Scalable multi-label canonical correlation analysis for cross-modal retrieval. *Pattern Recognition*, 115:107905, 2021.
- [2] Yan Gong, Georgina Cosma, and Hui Fang. On the limitations of visual-semantic embedding networks for image-to-text information retrieval. *Journal of Imaging*, 7(8):125, 2021.
- [3] Fartash Faghri, David J Fleet, Jamie Ryan Kiros, and Sanja Fidler. VSE++: improving visual-semantic embeddings with hard negatives. In *BMVC*, page 12, 2018.
- [4] Kuang-Huei Lee, Xi Chen, Gang Hua, Houdong Hu, and Xiaodong He. Stacked cross attention for image-text matching. In *ECCV*, pages 201–216, 2018.
- [5] Kunpeng Li, Yulun Zhang, Kai Li, Yuanyuan Li, and Yun Fu. Visual semantic reasoning for image-text matching. In *ICCV*, pages 4654–4662, 2019.
- [6] Jiacheng Chen, Hexiang Hu, Hao Wu, Yuning Jiang, and Changhu Wang. Learning the best pooling strategy for visual semantic embedding. In *CVPR*, pages 15789–15798, 2021.
- [7] Jacob Devlin, Ming-Wei Chang, Kenton Lee, and Kristina Toutanova. BERT: pre-training of deep bidirectional transformers for language understanding. In *NAACL*, pages 4171–4186, 2019.
- [8] Alec Radford, Jong Wook Kim, Chris Hallacy, Aditya Ramesh, Gabriel Goh, Sandhini Agarwal, Girish Sastry, Amanda Askell, Pamela Mishkin, Jack Clark, et al. Learning transferable visual models from natural language supervision. In *ICML*, pages 8748–8763, 2021.
- [9] Haoyu Ma, Handong Zhao, Zhe Lin, Ajinkya Kale, Zhangyang Wang, Tong Yu, Jiuxiang Gu, Sunav Choudhary, and Xiaohui Xie. El-CLIP: entity-aware interventional contrastive learning for e-commerce cross-modal retrieval. In *CVPR*, pages 18051–18061, 2022.
- [10] Tianyi Wei, Dongdong Chen, Wenbo Zhou, Jing Liao, Zhentao Tan, Lu Yuan, Weiming Zhang, and Nenghai Yu. HairCLIP: design your hair by text and reference image. In *CVPR*, pages 18072–18081, 2022.
- [11] Yiwu Zhong, Jianwei Yang, Pengchuan Zhang, Chunyuan Li, Noel Codella, Liunian Harold Li, Luowei Zhou, Xiyang Dai, Lu Yuan, Yin Li, et al. RegionCLIP: region-based language-image pretraining. In *CVPR*, pages 16793–16803, 2022.
- [12] Feiniu Yuan, Zhengxiao Zhang, and Zhijun Fang. An effective CNN and transformer complementary network for medical image segmentation. *Pattern Recognition*, 136:109228, 2023.
- [13] Pil-Soo Kim, Dong-Gyu Lee, and Seong-Whan Lee. Discriminative context learning with gated recurrent unit for group activity recognition. *Pattern Recognition*, 76:149–161, 2018.
- [14] Shaoqing Ren, Kaiming He, Ross Girshick, and Jian Sun. Faster R-CNN: towards real-time object detection with region proposal networks. *IEEE TPAMI*, 39(6):1137–1149, 2016.
- [15] Yu Liu, Yanming Guo, Li Liu, Erwin M Bakker, and Michael S Lew. CycleMatch: a cycle-consistent embedding network for image-text matching. *Pattern Recognition*, 93:365–379, 2019.
- [16] Qi Zhang, Jianlong Chang, Gaofeng Meng, Shibiao Xu, Shiming Xiang, and Chunhong Pan. Learning graph structure via graph convolutional networks. *Pattern Recognition*, 95:308–318, 2019.

[17] Kunpeng Li, Yulun Zhang, Kai Li, Yuanyuan Li, and Yun Fu. Image-text embedding learning via visual and textual semantic reasoning. *IEEE TPAMI*, 2022.

[18] Zhaoqing Wang, Yu Lu, Qiang Li, Xunqiang Tao, Yandong Guo, Mingming Gong, and Tongliang Liu. CRIS: CLIP-driven referring image segmentation. In *CVPR*, pages 11686–11695, 2022.

[19] Jing Yu, Zihao Zhu, Yujing Wang, Weifeng Zhang, Yue Hu, and Jianlong Tan. Cross-modal knowledge reasoning for knowledge-based visual question answering. *Pattern Recognition*, 108:107563, 2020.

[20] Bingqian Lin, Yi Zhu, and Xiaodan Liang. Atom correlation based graph propagation for scene graph generation. *Pattern Recognition*, 122:108300, 2022.

[21] Jie Cao, Shengsheng Qian, Huaiwen Zhang, Quan Fang, and Changsheng Xu. Global relation-aware attention network for image-text retrieval. In *ICMR*, pages 19–28, 2021.

[22] Guang Yang, Juan Cao, Zhineng Chen, Junbo Guo, and Jintao Li. Graph-based neural networks for explainable image privacy inference. *Pattern Recognition*, 105:107360, 2020.

[23] Yan Gong and Georgina Cosma. Improving visual-semantic embeddings by learning semantically-enhanced hard negatives for cross-modal information retrieval. *Pattern Recognition*, 137:109272, 2023.

[24] Junhua Mao, Jonathan Huang, Alexander Toshev, Oana Camburu, Alan L Yuille, and Kevin Murphy. Generation and comprehension of unambiguous object descriptions. In *CVPR*, pages 11–20, 2016.

[25] Justin Johnson, Bharath Hariharan, Laurens Van Der Maaten, Li Fei-Fei, C Lawrence Zitnick, and Ross Girshick. CLEVR: a diagnostic dataset for compositional language and elementary visual reasoning. In *CVPR*, pages 2901–2910, 2017.

[26] Peter Young, Alice Lai, Micah Hodosh, and Julia Hockenmaier. From image descriptions to visual denotations: new similarity metrics for semantic inference over event descriptions. *Transactions of the Association for Computational Linguistics*, 2:67–78, 2014.

[27] Tsung-Yi Lin, Michael Maire, Serge Belongie, James Hays, Pietro Perona, Deva Ramanan, Piotr Dollár, and C Lawrence Zitnick. Microsoft COCO: common objects in context. In *ECCV*, pages 740–755. Springer, 2014.

[28] Qi Zhang, Zhen Lei, Zhaoxiang Zhang, and Stan Z Li. Context-aware attention network for image-text retrieval. In *CVPR*, pages 3536–3545, 2020.

[29] Xi Wei, Tianzhu Zhang, Yan Li, Yongdong Zhang, and Feng Wu. Multi-modality cross attention network for image and sentence matching. In *CVPR*, pages 10941–10950, 2020.

[30] Gen Li, Nan Duan, Yuejian Fang, Ming Gong, and Dixin Jiang. Unicoder-VL: a universal encoder for vision and language by cross-modal pre-training. In *AAAI*, volume 34, pages 11336–11344, 2020.

[31] Yen-Chun Chen, Linjie Li, Licheng Yu, Ahmed El Kholy, Faisal Ahmed, Zhe Gan, Yu Cheng, and Jingjing Liu. UNITER: universal image-text representation learning. In *ECCV*, pages 104–120. Springer, 2020.

[32] Fei Yu, Jiji Tang, Weichong Yin, Yu Sun, Hao Tian, Hua Wu, and Haifeng Wang. ERNIE-ViL: knowledge enhanced vision-language representations through scene graphs. In *AAAI*, volume 35, pages 3208–3216, 2021.

[33] Mengjun Cheng, Yipeng Sun, Longchao Wang, Xiongwei Zhu, Kun Yao, Jie Chen, Guoli Song, Junyu Han, Jingtuo Liu, Errui Ding, et al. ViSTA: vision and scene text aggregation for cross-modal retrieval. In *CVPR*, pages 5184–5193, 2022.

[34] Zhe Gan, Yen-Chun Chen, Linjie Li, Chen Zhu, Yu Cheng, and Jingjing Liu. Large-scale adversarial training for vision-and-language representation learning. *Journal of Advances in neural information processing systems*, 33:6616–6628, 2020.

[35] Haoyu Lu, Nanyi Fei, Yuqi Huo, Yizhao Gao, Zhiwu Lu, and Ji-Rong Wen. COTS: collaborative two-stream vision-language pre-training model for cross-modal retrieval. In *CVPR*, pages 15692–15701, 2022.